IEEE Access
Multidisciplinary ⋮ Rapid Review ⋮ Open Access Journal

Received 18 October 2023, accepted 17 November 2023, date of publication 23 November 2023,
date of current version 4 December 2023.

Digital Object Identifier 10.1109/ACCESS.2023.3335932

RESEARCH ARTICLE

Total Energy Cost Optimization for Data Collection With Boat-Assisted Drone: A Study on Large-Scale Marine Sensor

XIANFEI HUANG[1] **AND GAOCAI WANG**[2]
[1]School of Electrical Engineering, Guangxi University, Nanning 530004, China
[2]School of Computer and Electronic Information, Guangxi University, Nanning 530004, China

Corresponding author: Gaocai Wang (wanggcgx@163.com)

This work was supported by the National Natural Science Foundation of China under Grant 62062007.

ABSTRACT Collecting broad ocean region data to leverage large-scale sensors is a valid method to handle ocean health problems associated with human activities (wind turbine deployment, nuclear wastewater discharge, etc.). When using the novel collection scheme, reducing the total energy consumption (TEC) of boat-assisted drones to collect sensor data is challenging. The objective of this study was to minimize the TEC of boats and drones (owing to their limited battery capacity) during marine environment sensor data collection. To achieve this, new models for drone hovering in wind, data collection, and related wireless communication have been developed, and the TEC minimization problem has been formulated as a new specialized distance-constrained capacitated vehicle routing problem. The problem is divided into four subproblems to reduce complexity. Based on these four subproblems, an improved heuristic algorithm was proposed. In the algorithm, the drone hovering position and boat waypoint are determined using the K-means clustering algorithm and the smallest enclosing circle algorithm. Based on the position and waypoint, the routes of drones and boats were optimized using the Lin-Kernighan heuristic 3 algorithm, thus minimizing the TEC. The simulation results demonstrate that when the boat waypoint is 3 and the sensor number is 2000, owing to the strong local and global search ability, the TEC in the scheme is 0.03×10^8J less than that of the graph attention neural network method (GANN), while the scheme also provides time saving, scalability, and flexibility.

INDEX TERMS Boat, drone, large-scale offshore sensors, optimization, total energy consumption.

NOMENCLATURE

A. SET AND INDICES

m,l	Boat waypoint index.
i,j	UAV hovering position index.
k	Sensor position index.
Φ	Set of boat waypoints.
M	Total number of boat waypoints.
$\mathcal{L}$	Set of UAV hovering positions.
I	Total number of hovering positions.
Λ	Set of sensor positions.

B. PARAMETERS

$v_{m,0}$	Boat waypoint.
$v_{m,i}$	UAV hovering position.
H_i	Average altitude of the UAV communication.
q_k	Sensor position.
$\mathcal{T}_\varphi$	Thrust of UAV.
mg	Weight of the UAV.
α	Tilt angle.
w	Wind speed.
μ	Empirically determined coefficient.
w_0	Basic wind speed.
h_0	Basic altitude.
δ	Earth's surface friction coefficient.
$P_{\mathrm{h}}(w)$	hovering power consumption.

The associate editor coordinating the review of this manuscript and approving it for publication was Adamu Murtala Zungeru.

$\boldsymbol{\Omega}$	Blade angular velocity.
$\mathrm{я}$	Rotor radius.
$\boldsymbol{\gamma}$	Incremental correction factor.
$\boldsymbol{d_0}$	Fuselage drag ratio.
$\boldsymbol{\rho}$	Air density.
$\boldsymbol{s}$	Rotor solidity.
a	Rotor disc area.
$\boldsymbol{\vartheta}$	Profile drag coefficient.
$\boldsymbol{d}^{\mathrm{p}}_{i,k}$	Plane distance between the sensor and the UAV.
$\boldsymbol{d}^{\mathrm{c}}_{i,k}$	Communication distance between the sensor and the UAV.
$\boldsymbol{g_{\mathrm{t}}}$	Channel power gain.
$\boldsymbol{\beta_0}$	Channel gain.
$\boldsymbol{\tau}$	Additional attenuation factor.
$\boldsymbol{\theta}$	Elevation angle.
$\boldsymbol{P}^{\mathrm{LoS}}_{i,k}(\boldsymbol{\theta})$	LoS probability.
$\boldsymbol{c}, \boldsymbol{d}$	Parameters of the propagation environment.
$\boldsymbol{R_{i,k}}$	Throughput between the sensor and UAV.
$\hat{\boldsymbol{g}}_t$	Random variable for small-scale fading.
$\boldsymbol{P_t}$	Transmission power.
$\boldsymbol{W}$	Bandwidth.
$\boldsymbol{\sigma^2}$	Noise power.
$\acute{\mathrm{R}}_{i,k}$	Approximate throughput.
$\boldsymbol{D_k}$	Data amount.
$\boldsymbol{P}_{\mathrm{c}}$	Communication-related power consumption.
$\boldsymbol{T_{i,k}}$	Transmit time.
$\boldsymbol{T}^{\mathrm{h}}_{i,k}$	UAV hovering time.
$\boldsymbol{K}$	Limitation number of sensors administered by the UAV.
$\boldsymbol{E}^{\mathrm{h}}_{i}$	UAV hovering energy consumption.
$\boldsymbol{P_{\mathrm{u}}}$	UAV power consumption under average wind speed.
$\boldsymbol{V_{\mathrm{U}}}$	UAV airspeed.
$\boldsymbol{E_{\mathrm{U}}}$	UAV energy consumption in data collection.
FD_L	Maximum travelling distance limitation of the UAV.
HT_L	Hovering time limitation of the UAV.
$\boldsymbol{E_{\mathrm{B}}}$	Boat energy consumption in data collection.
$\boldsymbol{V_{\mathrm{B}}}$	Speed of boat.
$\boldsymbol{P_{\mathrm{B}}}$	Power consumption of boat.
$\boldsymbol{N}$	Maximum number of trips.
$\boldsymbol{d}^{\mathrm{p}}_{m,l}$	Distance between the two boat waypoints.
$\boldsymbol{d}^{\mathrm{p}}_{i,j}$	Distance between the two hovering positions.
$\boldsymbol{E_{\mathrm{Uh}}}$	Total UAV hovering energy consumption.
$\boldsymbol{E_{\mathrm{Ut}}}$	Total UAV traveling energy consumption.

C. VARIABLES

$\boldsymbol{G^{\mathrm{B}}}$	Boat-planning graph.
$\mathfrak{Z}^{\mathrm{B}}$	The set of routes between any two boat waypoints.
$\boldsymbol{\eta_{m,l}}$	boat moves from the mth waypoint to the lth waypoint.
$\boldsymbol{G^{\mathrm{U}}}$	Complete UAV-planning graph.
$\mathfrak{Z}^{\mathrm{U}}$	The set of routes between any two boat waypoints.
$\boldsymbol{\xi_{i,n}}$	UAV collects data at hovering position $v_{m,i}$ in nth trip.
$\boldsymbol{\varsigma_{i,j,n}}$	UAV flies from the hovering position $v_{m,i}$ to the hovering position $v_{m,j}$ in nth trip.
$\boldsymbol{U_{i,k}}$	Binary variable for deciding the attribution.

I. INTRODUCTION

Deploying offshore wind turbines into the ocean undoubtedly has various effects on the marine environment, such as changes in water quality, sediment transport, marine ecology, and underwater noise [1]. As offshore wind resource development gradually extends to wide deep-sea areas [2], these impacts and the collection of related scientific exploration data of nuclear-polluted (or influenced/unknown) marine environments are increasing. Recent reports have shown that radioactive wastewater discharge into the environment remains a major concern for governments, researchers, and society [3], [4]. In the past decade, there have also been reports on the design of nanosensors for fissile materials in nuclear wastewater [5]. To acquire this scientific data, scholars have begun to apply ocean monitoring networks (OMNs) to collect related oceanic sensor data [6], [7]. The use of unmanned aerial vehicles (UAVs) to assist with data collection has become a popular research topic. In [7] and [8], Liu et al. regarded UAVs as data mules that collect data from underwater sensor nodes (USNs) via sea-surface sink nodes (SNs) within the OMNs framework. However, owing to the limitations of UAV batteries, UAV cannot hover or fly for extended periods [9]. Therefore, that UAV collects data from wide waters, especially from large-scale SNs in a wide deep sea is hard. However, battery charging stations for UAVs in a wide deep sea, along with an effective UAV path planning strategy to reduce the energy consumption of UAVs, are necessary [10]. It appears that some fixed charging stations are advisable. However, constructing and maintaining battery change stations in a wide deep sea is costly and fixed stations lack scalability and flexibility.

To address these limitations, inspired by a truck combined with a UAV in solving the delivery problem [9], we propose a novel scheme that uses a boat to assist the UAV in collecting sensor data from the large-scale sea surface sink nodes (SNs). In this scheme, the boat is outfitted with UAV battery-change stations, and can offer a takeoff and landing location for the UAV. Although boats have many benefits for UAV data collection, their energy consumption must be considered. In addition, according to [9], using the truck to combine with the UAV, the optimization objective should be changed to the integrated costs of the truck and UAV. Therefore, in this study, our objective was to optimize the total energy consumption (TEC) of boats and UAV. This approach adopts a comprehensive system design methodology in engineering practice that minimizes the number of unknown parameters [11]. The main contributions of this study are as follows.

- We propose a new boat-assisted UAV scheme for collecting large-scale offshore sensor data. This scheme enhances the scalability and flexibility of data

collection, particularly in the broader offshore and deep-sea regions.
- Wind conditions must be considered to reduce the energy consumption of the UAV. Therefore, we developed a new UAV hovering model and novel data collection and communication model.
- We formulated the total energy consumption problem of boats and UAV as a new special distance-constrained capacitated vehicle routing problem (DCVRP), aiming to minimize the TEC of both boats and UAV.
- To address the new DCVRP, we employed a new advanced heuristic algorithm, the Lin-Kernighan heuristic 3.0 (LKH-3), along with two other algorithms. This combination enhances the optimization capability of the proposed algorithm.
- By applying a mixed set of algorithms, we optimized the TEC of the data collection process, resulting in a significantly improved energy efficiency.

The remainder of this paper is organized as follows. Section II presents related research. Section III illustrates the system model, UAV hovering model, UAV data-collection model, problem formulation, solution method, and algorithm design. Section IV provides numerical simulation results, analysis, discussion, and performance evaluation. Section V provides concluding remarks.

II. RELATED WORK

With the recent advancements in offshore wind power technology and its expansion into the deep sea, wind facilities have gradually developed from nearby offshore locations to deep-sea areas [2]. Therefore, the influence of facilities on the deep sea, particularly the collection of related scientific exploration data, should be considered. More importantly, radioactive wastewaterdischarge into the environment remains a majorconcern for governments, researchers, and society [3], [4]. To collect these scientific data, UAVs have been utilized as data mules between SNs and ground base stations (GBS) [7]. This benefits from their flexible networking configurations and freedom from geographical restrictions [12]. However, the battery energy of UAV limits the hovering time and flying range during data collection. For the battery limitation challenge, the research [9] on the delivery data problem by UAV mentioned that the truck can be combined with the UAV, so the UAV can extend its flight range. In [13], Das proposed a scheme that combines drones and delivery trucks to act as mobile launching and retrieval sites for UAV. Ribeiro et al. [10] reported that UAV can be assisted by mobile charging stations during search-and-rescue missions. Obviously, in the deep sea area, the boat can also act as the mobile charging station, launching and recovery sites for drones, it is quite wonderful.

Using the boat instead of the truck as the mobile site for the UAV, the integrated cost of the boat (or truck) should be considered, including the time, traveling distance, and energy consumption. For example, Li et al. [9] introduced the two-echelon vehicle routing problem with time windows and mobile satellites (2E-VRP-TM) to solve the challenges they encountered. To address this challenge, they developed an adaptive large-neighborhood search heuristic and used it to effectively minimize the integrated costs. For an optimal delivery route, Das et al. [13] formulated a vehicle routing problem with time windows (VRPTW), similar to the job scheduling problem in their mechanism. To solve this problem, they proposed the collaborative Pareto ant colony algorithm (P-ACO). The proposed mechanism is an efficient solution for reducing integrated costs in parcel delivery logistics. Ribeiro et al. [10] presented a modified version of the vehicle routing problem (VRP) to address the combined utilization of UAVs and mobile charging stations. Using the construct-and-adjust heuristic method integrated with a genetic algorithm (GA), they offered an appealing planning approach to enhance the efficiency and speed of responses in search and rescue missions.

Considering the information presented in the aforementioned articles, it can be concluded that the heuristic algorithm is a suitable approach for addressing VRP and their variants. Consequently, for the distance-constrained capacitated vehicle routing problem (DCVRP) [14], which is another variant of VRP, the heuristic algorithm can also serve as an appropriate solution method. However, unlike the VRP, which is known to be NP-hard, the DCVRP is considered stronger NP-hard [14]. Therefore, it is essential to consider an improved heuristic algorithm with enhanced optimization capabilities. The LKH-3 algorithm is a well-suited heuristic algorithm for effectively addressing strongly NP-hard problems [15]. It was developed by Helsgaun based on the Lin-Kernighan heuristic (LKH) and the LKH did effective in the traveling salesman problem (TSP) [16]. LKH uses a 1-tree to define the alpha measure to determine the optimal solution. LKH-3 uses penalty functions to address these constraints. In contrast to LKH, the constraints are handled by the penalty functions in LKH-3. Meanwhile, to solve the VRP, in addition to GA and LKH-3, there are other state-of-the-art methods, including simulated annealing (SA) [17], [18], particle swarm optimization (PSO) [18], Tabu search (TS) algorithm [17], and graph attention neural network (GANN) [19]. However, GA is good at finding the optimal global solution, and it is difficult to find the optimal local solution. SA has a good local search ability, but it is difficult to find an optimal global solution. PSO has poor local search capability and its search accuracy is not sufficiently high. The TS is weak in determining the optimal global solution. Compared with the above algorithm, LKH-3 has a strong local search capability and global optimization ability. GANN also has a strong capability for local and global searches. However, the search solution ability of LKH-3 is slightly stronger than that of GANN. The disadvantage of LKH-3 is that its time complexity is higher than that of the GANN.

Wind speed also plays a crucial role in planning UAVs paths for ocean data collection [20]. Although the wind speed can vary over time [21], both on land and at sea, it is often

assumed to be constant when creating UAV flight paths [20], [22], [23] or during hovering. The adoption of the average wind speed in these studies is reasonable because data collection is typically avoided under strong-wind and heavy-rain conditions to prevent UAV accidents. However, during the data collection process, UAV may encounter random variations in wind speed, such as large, medium, or small changes; different wind directions; or even no wind. In such cases, obtaining the average wind value during UAV flight and hovering is a suitable approach to data collection.

According to the delivery problem, customer positions are key elements in path planning. In our research on large-scale SNs data collection, the UAV data-collection position was similar to the customer position. Therefore, it is important to determine its position. For example, Huang et al. [12] studied a UAV-assisted internet of things (IoT) data-collection system. To minimize system energy consumption, they exploited heuristic evolutionary algorithms to solve the UAV deployment position problem. Xu et al. [24] addressed the issue of unreasonable distribution of UAV data collection positions because it results in a high TEC for IoT systems. They utilized a differential evolution algorithm with variable population sizes based on a mutation strategy pool initialized by the K-means clustering algorithm to minimize the energy consumption of the system during data transmission by optimizing the UAV positions. The K-means clustering algorithm is a method based on the Euclidean distance, where neighborhood points are gathered together as much as possible, and the non-neighborhood points are separated as far as possible. Therefore, this is a better algorithm for solving the minimum communication distance between UAV and IOT devices. Reference [24] reported that the shorter the distance, the smaller the energy consumption of communication. Meanwhile, to optimize the energy consumption of communication between the UAV and IOT device, another algorithm can be chosen, that is, the smallest enclosed circle (SEC) algorithm, which finds the minimum circle from multiple scatters to cover these scatters. The radius of the minimum circle is the minimum communication distance between the UAV and the IOT devices.

III. SYSTEM MODELS AND METHODS

A. SYSTEM MODELS

An example scenario for the data collection of large-scale sea surface sensors using a boat-assisted UAV is shown in Figure 1. The waypoint of the boat is indicated by $v_{m,0} = [x_m, y_m]$, $v_{m,0} \in \Phi$, $m \leq M, M$ boat waypoints are in set Φ. The UAV hovering position is denoted by $v_{m,i} = [x_i, y_i], v_{m,i} \in \mathcal{L}$, $i \neq 0, i \leq I$. There are I hovering positions of the UAV in set $\mathcal{L}$. Let the average altitude of the UAV communication state be H_i, meanwhile be at the hovering position $v_{m,i}$. The horizontal location of the wireless sensor is denoted as $q_k = [x_k, y_k], q_k \in \Lambda$, where Λ denotes the set of sensors.

1) THE UAV HOVERING MODEL

When the maritime UAV collects data, it encounters random wind speed at any hovering position $v_{m,i}$. As shown in Figure 2, we consider a UAV hovering model. The thrust $\mathcal{T}_\varphi$ of a UAV is expressed as

$$\mathcal{T}_\varphi \cos\alpha = mg, \tag{1}$$

where α is the tilt angle between the vector of $\mathcal{T}_\varphi$ and the inverse direction vector of mg, which is the weight of the UAV using Newton as a unit. The α can be obtained from [25]

$$\alpha = \arctan\left(w^2/\mu\right), \tag{2}$$

where w is the wind speed and μ is an empirically determined coefficient [25]. Therefore, the relationship between the thrust $\mathcal{T}_\varphi$ and wind speed w is expressed as

$$\mathcal{T}_\varphi = {}^{mg}/_{\cos\left(\arctan\left(w^2/\mu\right)\right)}. \tag{3}$$

Because the wind speed change with altitude, at a hovering position $v_{m,i}$, we have

$$w(H_i) = w_0 \left({}^{H_i}/_{h_0}\right)^{\delta}, \tag{4}$$

where w_0 is the basic wind speed, h_0 is the basic altitude, and δ is Earth's surface friction coefficient. Therefore, the hovering power consumption $P_{\mathrm{h}}(w)$ of the UAV using Watt (W) as a unit is decomposed as [25], [26]

$$\begin{cases} P_{\mathrm{h}}\left(w(H_i)\right) = \vartheta \rho s \Omega^3 \text{я}^3 \dfrac{\text{д}}{8} + (1+\gamma)\,\mathcal{T}_\varphi\,(H_i)^{3/2}/\sqrt{2\rho\text{д}} \\ \mathcal{T}_\varphi\,(H_i) = {}^{mg}/_{\cos\left(\arctan\left(w(H_i)^2/\mu\right)\right)}, \end{cases} \tag{5}$$

where Ω is the blade angular velocity, я is the rotor radius, γ is the incremental correction factor to the induced power, and $d_0, \rho,$ and s present the fuselage drag ratio, the air density, and the rotor solidity, respectively. д stands for the rotor disc area. ϑ indicates the profile drag coefficient.

2) THE UAV DATA COLLECTION MODEL

A wireless communication model used for the rotary-wing UAV collecting sensor data is shown in Figure 3 (each deep blue area in Figure 1). The plane distance between the sensor and UAV is $d^{\mathrm{p}}_{i,k} = \left|\left|v_{m,i} - q_k\right|\right|, q_k \in \Lambda$. The communication distance between the sensor and UAV is expressed as $d^{\mathrm{c}}_{i,k} = \sqrt{{H_i}^2 + \left(d^{\mathrm{p}}_{i,k}\right)^2}, q_k \in \Lambda$. The path loss is proportional to the communication distance but inversely proportional to the channel power gain [17]. For sensor-UAV links, large-scale attenuation is usually modeled as a random variable depending on the occurrence probabilities of the line-of-sight (LoS) links and non-line-of-sight (NLoS) links [26], [27]. Thus, based on [17], [26], and [27], especially considering the interference-free scenario (rural and suburban) [28] or even the sea environment, the channel power gain is given as g_{t}, which can be written as

$$g_{\mathrm{t}} = \begin{cases} \beta_0 \left(d^{\mathrm{c}}_{i,k}\right)^{-2}, & \text{LoS link}, \\ \tau\beta_0 \left(d^{\mathrm{c}}_{i,k}\right)^{-2}, & \text{NLoS link}, \end{cases} \tag{6}$$

where β_0 is the channel gain at a reference distance and that $\tau < 1$ is the additional attenuation factor owing to the NLoS

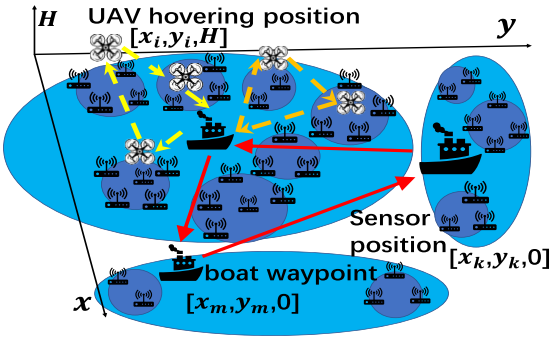

FIGURE 1. The example scenario for boat-assisted unmanned vehicle aircraft (UAV) collecting sensor data on the ocean environment.

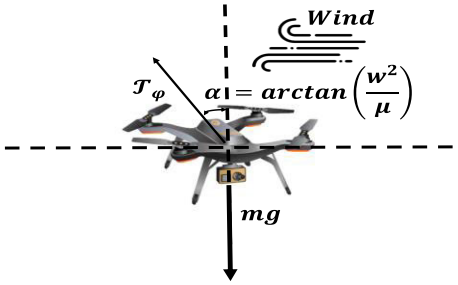

FIGURE 2. An unmanned vehicle aircraft (UAV) hovering energy consumption model with wind condition.

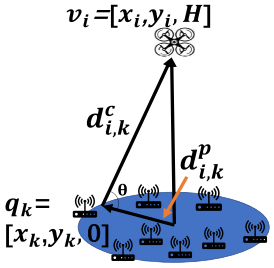

FIGURE 3. The unmanned vehicle aircraft (UAV) sensor data collection model for the ocean environment.

condition. The probability that occurs in the LoS propagation group depends on the propagation environment and elevation angle θ. Therefore, the LoS probability is denoted as $P^{\mathrm{LoS}}_{i,k}(\theta)$, which can be expressed in the following form [28] and [29],

$$P^{\mathrm{LoS}}_{i,k}(\theta) = 1/(1+c\exp(-d[\theta-c]))\,, \tag{7}$$

where c and d are related directly to the propagation environment. θ indicates the elevation angle related to the UAV average communication altitude H_i and the plane distance $d^{\mathrm{p}}_{i,k}$, that is, $\theta = \arctan\left(H_i/d^{\mathrm{p}}_{i,k}\right)$.Usually, considering only the locations of the UAVs and devices, it is difficult to determine exactly which path loss type (LoS/NLoS) is experienced by the device-UAV link [30]. Therefore, by averaging over the randomness of both LoS and NLoS links [17], [30], the expected channel power gain can be calculated as

$$\begin{aligned}\mathbb{E}\left[g_{\mathrm{t}}\right]_{i,k} &= P^{\mathrm{LoS}}_{i,k}(\theta)\,\beta_0\left(d^{\mathrm{c}}_{i,k}\right)^{-2} \\ &+ \left(1-P^{\mathrm{LoS}}_{i,k}(\theta)\right)\tau\beta_0\left(d^{\mathrm{c}}_{i,k}\right)^{-2}.\end{aligned} \tag{8}$$

In a time-division multiple access (TDMA) system, $R_{i,k}$ denote the throughput between the sensor and UAV. Similar to the methods in [26], for throughput calculation using Jensen's inequality, the expected communication throughput can be expressed as

$$\begin{aligned}\mathbb{E}\left[R_{i,k}\right] &= \mathbb{E}\left[W\log_2\left(1+{}^{P_{\mathrm{t}}g_{\mathrm{t}}\hat{g}_{\mathrm{t}}}/\sigma^2\right)\right], \\ &\leq \acute{\mathrm{R}}_{i,k} = W\log_2\left(1+{}^{P_{\mathrm{t}}\mathbb{E}[g_{\mathrm{t}}]_{i,k}}/\sigma^2\right),\end{aligned} \tag{9}$$

where $\hat{g}_{\mathrm{t}}$ is a random variable, and $\mathbb{E}\left[\hat{g}_{\mathrm{t}}\right] = 1$ accounts for small-scale fading [26], [28]. $\acute{\mathrm{R}}_{i,k}$ is the approximate throughput for $\mathbb{E}\left[R_{i,k}\right]$ [26], P_{t} is the transmission power, W is the bandwidth, and σ^2 is the noise power. Similar to [24], we assume that the kth sensor has a D_k amount of data sent to the UAV, and the time required to transmit the data from the kth sensor to the UAV at the hovering position $v_{m,i}$ is calculated by

$$T_{i,k} = D_k/\acute{\mathrm{R}}_{i,k}, \tag{10}$$

where $i \in I,\ q_k \in \Lambda$.

Each sensor can only send data to one UAV, and because of the system bandwidth limitations of the multiplexing measure used in [24], each UAV can only simultaneously receive data from up to K sensors. Thus, according to the number of hovering positions, the sensor set Λ can be divided into I subsets $\{\Lambda_1,\cdots,\Lambda_i\cdots,\Lambda_I\}$. The sensor's amount of any subset in these subsets is not more than K. At the hovering position $v_{m,i}$, the UAV needs to hover above the sensor subset Λ_i for a duration because the UAV must entirely collect all sensors' data in the subset Λ_i.

So, the UAV hovering time at the hovering position $v_{m,i}$ is as

$$T^{\mathrm{h}}_{i,k} = \max_{i\in I}\left\{T_{i,1},\cdots,T_{i,k},\cdots\right\}, \tag{11}$$

where $q_k \in \Lambda_i, k \leq K$.

The hovering energy consumption of the UAV at the ith hovering position is expressed as

$$E^{\mathrm{h}}_i = P_{\mathrm{h}}\left(w(H_i)\right)T^{\mathrm{h}}_{i,k}, \tag{12}$$

where $i \in I, q_k \in \Lambda_i$.

Let P_{c} denote communication-related power consumption; then, the hovering energy consumption of the UAV can be rewritten as

$$E^{\mathrm{h}}_i = \left(P_{\mathrm{h}}\left(w(H_i)\right)+P_{\mathrm{c}}\right)T^{\mathrm{h}}_{i,k}, \tag{13}$$

where $i \in I, q_k \in \Lambda_i$.

B. PROBLEM FORMULATION

In the process of collecting large-scale amounts of sensor data and optimizing the total energy consumption of the UAV and boat, routes were planned for both the UAV and boat. Figure 1 illustrates the planned route for the boat, which is represented

by the red line. There were multiple waypoints along this route. Each boat waypoint corresponds to a partitioned sub-region for data collection, as depicted by the blue areas.

When collecting data in each subregion, the UAV must perform multiple circular collection paths, as indicated by the green dotted-line loop. This circular collection process was repeated several times within a subregion to complete the data collection task considering the limited energy resources of the UAV. Subsequently, the UAV was transported by boat to the next sub-region for further data collection. It is important to note that each boat waypoint serves as a takeoff and landing location for UAV.

We first process the minimization problem of the boat's energy consumption (E_{B}) and the UAV's energy consumption (E_{U}), and then conveniently optimize the boat and UAV's TEC. We define a complete boat-planning graph $G^B = \{\Phi, \mathfrak{Z}^B\}$, then Φ and $\mathfrak{Z}^B$ denote the set of boat waypoints and set of routes between any two boat waypoints, respectively. The distance between the two waypoints is expressed as $d^{\mathrm{p}}_{m,l} = ||v_{m,0} - v_{l,0}||$, $v_{m,0}, v_{l,0} \in \Phi$. We use a binary variable η to denote the routes in $\mathfrak{Z}^B$. $\eta_{m,l} = 1$ when the boat moves from the mth waypoint to the lth waypoint. Otherwise, $\eta_{m,l} = 0$. The boat visited each waypoint once. Let V_{B} and P_{B} denote the velocity and power consumption of the boat, respectively. We have minimization problem 1 regarding the boat's energy consumption (E_{B})

(Problem 1)

$$\min E_{\mathrm{B}} = \sum_{m=0}^{|\Phi|} \sum_{l=0}^{|\Phi|} d^{\mathrm{p}}_{m,l} \eta_{m,l} P_{\mathrm{B}} / V_{\mathrm{B}}, \tag{14}$$

Subject to

$$\sum_{l=1,l\neq 0}^{|\Phi|} \eta_{0,l} = 1, \quad \sum_{l=1,l\neq 0}^{|\Phi|} \eta_{l,0} = 1, \tag{14a}$$

$$\sum_{m=0,l\neq m}^{|\Phi|} \eta_{m,l} = 1, \quad \sum_{l=0,l\neq m}^{|\Phi|} \eta_{l,m} = 1, \tag{14b}$$

$$\sum_{m\in S_{\mathrm{B}}} \sum_{l\in S_{\mathrm{B}}} \eta_{m,l} \leq |S_{\mathrm{B}}| - 1,$$
$$\forall S_{\mathrm{B}} \subset F, \ 2 \leq |S_{\mathrm{B}}| \leq |\Phi| - 1, \tag{14c}$$

where S_{B} denotes a subset of Φ. (14a) indicates that the boats' starting and ending places are both waypoints $v_{0,0}$. (14b) ensures that only one path exists between the mth and the lth boat waypoint. (14c) states that only one trip (red line in Figure 1) occurs in boat waypoint set Φ.

Because the boat waypoint ($v_{m,0}$) is the UAV takeoff and landing location, the quantity and distribution of boat waypoints influence the energy consumption of the boat and UAV. Therefore, we partition the hovering position set $\mathcal{L}$ into M subsets $\{\mathcal{L}_1, \cdots, \mathcal{L}_m, \cdots, \mathcal{L}_M\}$, and define a complete UAV-planning graph $G^{\mathrm{U}} = \{\{v_{m,0}, \mathcal{L}_m\}, \mathfrak{Z}^{\mathrm{U}}\}$, where $\mathcal{L}_m = \{v_{m,1}, \cdots, v_{m,i}, \cdots, v_{m,j}\}$. The UAV visits each hovering position only once, and the hovering time is $T^{\mathrm{h}}_{i,k}$. We define a binary variable as ξ, when the UAV collects data at hovering position $v_{m,i}$ in nth trip, $\xi_{i,n}$=1. Otherwise, $\xi_{i,n} = 0$. The maximum number of trips is N. Regard the boat waypoint $v_{m,0}$ as a hovering position ($T^{\mathrm{h}}_{0,k} = 0$) and insert it into the $\mathcal{L}_m$(i.e., $\mathcal{L}_m = \{v_{m,0}, v_{m,1}, \cdots, v_{m,i}, \cdots, v_{m,j}\}$), the distance between the two hovering positions is expressed as $d^{\mathrm{p}}_{i,j} = ||v_{m,i} - v_{m,j}||$. $\mathfrak{Z}^{\mathrm{U}}$ is a set of routes between any two boat waypoints. $\varsigma_{i,j,n} = 1$ when the UAV flies from hovering position $v_{m,i}$ to hovering position $v_{m,j}$ in nth trip. Otherwise, $\varsigma_{i,j,n} = 0$. The UAV takes off from $v_{m,0}$, and before the battery energy drains, it returns to $v_{m,0}$. Because of the battery energy limitation, the UAV's maximum hovering time and longest flight distance are HT_L and FD_L, respectively. According to [20], to calculate the flight energy consumption, let V_{U} and P_{u} denote the airspeed of the UAV and the power consumption under average wind speed, respectively. To optimize the total energy consumption of the UAV (E_{U}), we have Problem 2

(Problem 2)

$$\min E_{\mathrm{U}} = P_{\mathrm{u}} \sum_{m=1}^{M} \sum_{n=1}^{N} \sum_{i=0}^{|\mathcal{L}_m|} \sum_{j=0}^{|\mathcal{L}_m|} d^{\mathrm{p}}_{i,j} \varsigma_{i,j,n} / V_{\mathrm{U}} + \sum_{m=1}^{M} \sum_{n=1}^{N} \sum_{i=0}^{|\mathcal{L}_m|} E^{\mathrm{h}}_i \xi_{i,n}, \tag{15}$$

Subject to

$$\sum_{i=0}^{|\mathcal{L}_m|} T^{\mathrm{h}}_{i,k} \xi_{i,n} \leq \mathrm{HT}_L, \quad n = 1, \cdots, N, \tag{15a}$$

$$\sum_{i=0}^{|\mathcal{L}_m|} \sum_{j=0}^{|\mathcal{L}_m|} d_{i,j} \varsigma_{i,j,n} \leq \mathrm{FD}_L, \quad n = 1, \cdots, N, \tag{15b}$$

$$\sum_{n=1}^{N} \xi_{i,n} = \begin{cases} 1, & i = 1, \cdots, |\mathcal{L}_m| \\ N, & i = 0, \end{cases} \tag{15c}$$

$$\sum_{i=0}^{|\mathcal{L}_m|} \varsigma_{i,j,n} = \xi_{i,n}, \quad j = 1, \cdots, |\mathcal{L}_m|, \tag{15d}$$

$$\sum_{j=0}^{|\mathcal{L}_m|} \varsigma_{i,j,n} = \xi_{i,n}, \quad i = 1, \cdots, |\mathcal{L}_m|, \tag{15e}$$

where the two terms in (15) represent the total flight and hovering energy consumptions, respectively. (15a) and (15b) are the two constraints of the UAV in one data collection trip. During the entire data collection, (15c), (15d), and (15e) ensured that each hovering position was visited by the UAV only once.

In summary, the total energy consumption for boat-assisted UAV data collection under the newly developed DCVRP is expressed as

$$\min_{v_{m,0}, v_{l,0} \in F, v_{m,i}, v_{m,j} \in \mathcal{L}} E_{\mathrm{B}} + E_{\mathrm{U}}. \tag{16}$$

Based on the energy consumption of the boat and the energy consumption composition in Equation (16), it is crucial to determine the waypoint of the boat.

C. METHOD OF SOLVING PROBLEM

To solve (16), it is decomposed into four subproblems, as follows:

1) MINIMIZING THE UAV COLLECTION TIME FOR THE SUBSET DATA

With respect to sensor subset Λ_i is concerned, according to (11), there is a maximum data collection time $T^{\mathrm{h}}_{i,k}$ and a corresponding hovering position v_i in each subset. The UAV

must hover at position v_i for duration $T^{\mathrm{h}}_{i,k}$. Therefore, the minimum hovering time problem is expressed as

(Problem 3)

$$\min_{i\in I,k\in\Lambda_i} \max\left\{T_{i,1},\cdots,T_{i,k},\cdots\right\}. \tag{17}$$

So, to solve Problem 3, we have Proposition 1:

Proposition 1:

If a minimum exists in the $T^{\mathrm{h}}_{i,k}$, $i\in I$, $k\in\Lambda_i$, it is the only minimum of the function in $T^{\mathrm{h}}_{i,k}$.

Proof: According to the theory of the smallest enclosing circle, a final minimum enclosing circle has two properties: one is the circle being unique and the other is that the circle has only two cases:1. There are at least three points on the circle and the circle is restricted by three points (three points of the co-circle). 2. If there are only two points on the circle, it must have a line joining the two points as the diameter. Therefore, the radius of the final minimum enclosing circle is unique. In Λ_i, when the center of the circle is used as a sea surface point corresponding to the UAV hovering position, its radius is certainly the minimum plane distance $d^{\mathrm{p}}_{i,k}$ between the wireless sensor location and point (Figure 3).

According to (9), (10), and $d^{\mathrm{c}}_{i,k} = \sqrt{{H_i}^2+\left(d^{\mathrm{p}}_{i,k}\right)^2}$, we have

$$T_{i,k} = D_k/\acute{\mathrm{R}}_{i,k}(d^{\mathrm{p}}_{i,k}), \tag{18}$$

where the throughput $\acute{\mathrm{R}}_{i,k}(d^{\mathrm{p}}_{i,k})$ is a function of $d^{\mathrm{p}}_{i,k}$. Function is an increasing function of $d^{\mathrm{p}}_{i,k}$. Thus, the $T_{i,k}$ have unique minima.

2) MINIMIZING THE TOTAL UAV HOVERING ENERGY CONSUMPTION

Based on Problem 3, considering the relationship between the minimum plane distance $d^{\mathrm{p}}_{i,k}$ and the minimization problem of the total hovering energy consumption, this problem can be expressed as

(Problem 4)

$$\min_{i\in I,k\in\Lambda_i\subset\Lambda} E_{\mathrm{Uh}} = \min\sum\nolimits_{m=1}^{M}\sum\nolimits_{n=1}^{N}\sum\nolimits_{i=0}^{|\mathcal{L}_m|} E^{\mathrm{h}}_i\xi_{i,n}, \tag{19}$$

Subject to

$$|\Lambda_i|\le K, \tag{19a}$$

where (19a) indicates that each UAV can only receive data from up to K sensors simultaneously.

According to (13) and (18), E^{h}_i is related to the plane distance $d^{\mathrm{p}}_{i,k}$ between the center of the circle and the sensor in Λ_i, that is, $E^{\mathrm{h}}_i = \frac{(P_{\mathrm{h}}(w(H_i))+P_{\mathrm{c}})D_k}{\acute{\mathrm{R}}_{i,k}(d^{\mathrm{p}}_{i,k})}$. The function $E^{\mathrm{h}}_i = \mathrm{f}\left(d^{\mathrm{p}}_{i,k}\right)$, it is defined as a strictly monotonically increasing function. Thus, Problem 3 is simplified to the problem of the minimum sum of communication distances. Euclidean distance (i.e., $d^{\mathrm{p}}_{i,k} = \left|\left|v_{m,i}-q_k\right|\right|$) was used as the judgment criterion. Regarding the Euclidean distance, because using the distance or square of the distance does not affect the judgment criterion, the summation of the square of the distance was used as the objective function. Thus, we have Problem 5

(Problem 5)

$$\min\sum\nolimits_{i\in I}^{I}\sum\nolimits_{k\in\Lambda_i}^{\Lambda_i} U_{i,k}\left|\left|v_{m,i}-q_k\right|\right|^2, \tag{20}$$

Subject to

$$U_{i,k} = \begin{cases} 1, & i=\{i|\arg\min\left|\left|v_{m,i}-q_k\right|\right|\},\\ 0, & \text{otherwise}, \end{cases} \tag{20a}$$

where constraint (20a) indicates that q_k belongs to the nearest center point $v_{m,i}$ (the UAV hovering position). Problem 5 was a clustering problem. Based on Problem 5, Problem 4 can be rewritten as

(Problem 4a)

$$\min\sum\nolimits_{i\in I}^{I}\sum\nolimits_{k\in\Lambda_i}^{\Lambda_i} E^{\mathrm{h}}_i\left(\left|\left|v_{m,i}-q_k\right|\right|\right), \tag{21}$$

Subject to

$$|\Lambda_i|\le K, \tag{21a}$$

$$U_{k,i} = \begin{cases} 1, & i=\{i|\arg\min\left|\left|v_{m,i}-q_k\right|\right|\},\\ 0, & \text{otherwise}, \end{cases} \tag{21b}$$

Thus, the K-means clustering algorithm and SEC algorithm can be introduced to solve Problem 4a.

3) MINIMIZING THE TOTAL UAV TRAVELING ENERGY CONSUMPTION

To minimize the total traveling energy consumption E_{Ut} of the UAV during large-scale sensor data collection, the minimum problem is expressed as

(Problem 6)

$$\min E_{\mathrm{Ut}} = \min P_{\mathrm{u}}\sum\nolimits_{m=1}^{M}\sum\nolimits_{n=1}^{N}\sum\nolimits_{i=0}^{|\mathcal{L}_m|}\sum\nolimits_{j=0}^{|\mathcal{L}_m|} d^{\mathrm{p}}_{i,j}\varsigma_{i,j,n}/V_{\mathrm{U}}, \tag{22}$$

Subject to

$$(15a)-(15e).$$

Based on these constraints, Problem 6 was transformed into a DCVRP. Thus, Problem 6 was NP-hard. The methods for solving the DCVRP are diverse and can be used with any heuristic algorithm as follows: LKH-3, GA, ACO, SA, and PSO. Here, we use LKH-3 to find a promising DCVRP solution to conveniently address Problem 6.

4) MINIMIZING THE BOAT TRAVELING ENERGY CONSUMPTION

Problem 1 is a simple TSP problem (red line in Figure 1). However, the size of Problem 1 increases with an increase in the scale of set Φ in Figure 1.

To address the above problems, the following algorithms were designed and applied.

Algorithm 1 K-Means Clustering Algorithm

input: Λ, M, I
output: $\{v_{1,1}, \cdots, v_{m,i}, \cdots, v_{1,I}\}, \{\Lambda_1, \cdots, \Lambda_I\}$
1. Initialize the cluster centers $\{v_{1,1}, \cdots, v_{m,i}, \cdots, v_{1,I}\}$ randomly;
2. while $\{v_{1,1}, \cdots, v_{1,i}, \cdots, v_{1,I}\}$ no more change
3. Decide q_k belong to which $v_{m,i}$ by $||v_{m,i} - q_k||^2$;
4. Update $v_{m,i}$ by $v_{m,i} = \sum_{k\in\Lambda_i}^{\Lambda_i} U_{k,i} q_k / \sum_{k\in\Lambda_i}^{\Lambda_i} U_{k,i}$;
5. end
6. Return the cluster centers $\{v_1, \cdots, v_I\}$ and the subsets $\{\Lambda_1, \cdots, \Lambda_I\}$

Algorithm 2 SEC Algorithm

input: Λ, K
output: $\{v_{1,1}, \cdots, v_{1,i}, \cdots, v_{1,I}\}$
1. for i= 1 to I
2. Select any three sensors $\{q_{k-2}, q_{k-1}, q_k\}$
3. Obtain the smallest circle $C_{\acute{k}}$ that covered these sensors
4. While q_{k+1} is outside the $C_{\acute{k}}$
5. Update $C_{\acute{k}}$ by $C_{\acute{k}+1}$ and q_{k+1}
6. Update q_{k+1} by q_{k+2}
7. end
8. Obtain $v_{1,i}$ from $C_{\acute{k}}$.
9. end

D. ALGORITHM DESIGN FOR SOLVING PROBLEM

Based on Problems 1, 4a, and 6, we developed a new comprehensive algorithm based on the heuristic algorithm to solve (16), that is, the mixed double K-means and Lin–Kernighan heuristic algorithm (MDK-LKH). It includes the following three algorithms: The Lin-Kernighan heuristic algorithm, K-means clustering algorithm, and SEC algorithm [31]. In the proposed algorithms, to solve the minimum total energy consumption problem, it is crucial to obtain the optimal hovering position of the UAV that is similar to the optimal position of the boat waypoint. Therefore, we first determined the optimal hovering position using the SEC and K-means algorithms. LKH-3 is then introduced to solve Problem 6. LKH-3 is the solver, and its details are provided in [15]. Finally, TEC was addressed using MDK-LKH.

1) ALGORITHM 1: K-MEANS ALGORITHM

One of the methods used to find the hovering position of the UAV in large-scale data collection is the K-means clustering algorithm. Details of the K-means algorithm are presented in Algorithm 1.

In Algorithm 1, first, according to the number of boat waypoints I, the cluster centers (hovering positions) are randomly initialized according to the number of boat waypoints I. Then, the initial cluster centers $v_{m,i}$ are used in the iteration, and they are used to decide the attribution of the sensor. Subsequently, the cluster centers are updated in Line 4. When the new cluster centers are the same as the old ones, the iteration is stopped.

2) ALGORITHM 2: SEC ALGORITHM

As discussed in Proposition 1, for each subset Λ_i, there is a minimum UAV hovering time ($T^{\mathrm{h}}_{i,k}$) for the data collection. While the $T^{\mathrm{h}}_{i,k}$ is related to the plane distance $d^{\mathrm{p}}_{i,k}$ and the maximum number of sensors taken in charge via a UAV. Thus, by calculating $T^{\mathrm{h}}_{i,k}$ is transformed into looking for the minimum circle plane covering the entire sensor of this circle, and then the center of the circle (corresponding to the UAV hovering position) is obtained. Therefore, the SEC algorithm (Algorithm 2) is used to perform this task. The details are as follows.

In Algorithm 2, first, to select, check and confirm any three sensor locations $\{q_{k-2}, q_{k-1}, q_k\}$ in Λ_i, whether it forms a minimum circle C_k that covers whole sensors. Otherwise, another sensor location, q_{k+1} is selected for verification. When the sensor location q_{k+1} is outside the minimum circle C_k, the minimum circle is updated to cover the sensor locations $\{q_{k-2}, q_{k-1}, q_k, q_{k+1}\}$, and the next sensor location q_{k+2} is selected to obtain the minimum circle again. By using this iterative approach, the minimum circle covering the entire sensor in Λ_i can be obtained. All centers of the found minimum circles are used as the UAV corresponding to hovering positions in air, and each circle radius acts as the plane radius ($d^{\mathrm{p}}_{i,k}$) that corresponds to the communication distance $\left(d^{\mathrm{c}}_{i,k}\right)$ between the UAV and the sensor.

3) ALGORITHM 3: MDK-LKH DESIGN AND TIME COMPLEXITY ANALYSIS

To solve the TEC under the new special DCVRP, that is, (16), the designed MDK-LKH is exploited, and its details are as follows:

- The UAV hovering positions were obtained using the K-means clustering and SEC algorithms. Then, the set ($\mathcal{L}$) of hovering positions is split into multiple subsets, $\mathcal{L}_m$. The takeoff and landing locations of the UAV in the subsets are the waypoints of the boat. These were obtained using a K-means clustering algorithm.
- For each subset $\mathcal{L}_m$, the UAV hovering energy consumption in one subset was first obtained via the plane distance $d^{\mathrm{p}}_{i,k}$, and the total hovering energy consumption was subsequently obtained (i.e., Problem 4a).
- For each subset $\mathcal{L}_m$, via the plane distance $d^{\mathrm{p}}_{i,j}$, under the constraints of HT_L and FD_L, the summation of the UAV traveling energy consumption in one subset is obtained by LKH-3, and the total UAV traveling energy consumption used for data collection is acquired (i.e., Problem 6).
- The TSP travel distance of the boat was obtained using the LKH (Problem 1). Thus, the boat-traveling energy consumption was also obtained.
- Finally, the TEC was obtained by minimizing the sum of the boat-traveling energy consumption and the total energy consumption of the UAV.

Thus, the detail is given in Algorithm 3.

For the K-means clustering algorithm, we assumed that iter is the number of iterations. The time complexity of the K-means Algorithm is $O(2I\,|\Lambda|\,\mathrm{iter})$ in Line 1. Similarly, the

Algorithm 3 Mixed Double K-Means and Lin-Kernighan Heuristic Algorithm

input: Λ, K, M
output: $E_{\mathrm{B}} + E_{\mathrm{U}}$
1. The optimal hovering positions in the set $\mathcal{L}$ are obtained by K-means algorithm and SEC algorithm
2. The subsets $\{\mathcal{L}_1, \cdots, \mathcal{L}_M\}$ are obtained by K-means algorithm
3. The boat waypoints $\{v_{1,0}, \cdots, v_{M,0}\}$ are obtained by K-means algorithm
4. for $i = 1$ to M
5. Obtain the minimum sum of UAV traveling distances $\sum_{n=1}^{N} \sum_{i=0}^{|\mathcal{L}_m|} \sum_{j=0}^{|\mathcal{L}_m|} d_{i,j}^{\mathrm{p}} \varsigma_{i,j,n}$ by LKH-3 with $v_{m,0}$, $\mathcal{L}_m$, $\mathrm{HT_L}$, and $\mathrm{FD_L}$
6. Record $\sum_{n=1}^{N} \sum_{i=0}^{|\mathcal{L}_m|} \sum_{j=0}^{|\mathcal{L}_m|} d_{i,j}^{\mathrm{p}} \varsigma_{i,j,n}$
7. end
8. Obtain the minimum boat energy consumption E_{B} of the boat by the LKH
9. $\min \ E_{\mathrm{B}} + E_{\mathrm{U}} \leftarrow \min P_{\mathrm{B}} \sum_{m=0}^{|\Phi|} \sum_{l=0}^{|\Phi|} d_{m,l}^{\mathrm{p}} \eta_{m,l} / V_{\mathrm{B}} + P_{\mathrm{u}} \sum_{n=1}^{N} \sum_{i=0}^{|\mathcal{L}_m|} \sum_{j=0}^{|\mathcal{L}_m|} d_{i,j}^{\mathrm{p}} \varsigma_{i,j,n} / V_{\mathrm{U}} + \sum_{m=1}^{M} \sum_{n=1}^{N} \sum_{i=0}^{|\mathcal{L}_m|} E_i^{\mathrm{h}} \xi_{i,n}$.

time complexity in Line 2 is $O(2M\,|\mathcal{L}|\,\mathrm{iter})$, where $|\mathcal{L}| = I$. According to [31], the time complexity of the SEC algorithm is $O\left(I \lg \frac{m_d}{R_{\mathrm{a}}}\,|\Lambda_i|\right)$, where m_d is the shortest distance from a circle-round outside point to the circumference of the circle. R_{a} is the radius of the smallest enclosing circle obtained in the last iteration.

In Problem 6, the time complexity of LKH-3 can be simplified to $O\left(|\mathcal{L}_m|^2\right)$. Problem 1 is similar to Problem 6, and the time complexity of the solution to Problem 1 is $O\left(M^2\right)$. In other words, LKH-3 must be run M times in MDK-LKH. Based on the above discussion, the time complexity of MDK-LKH is $O(2I\,|\Lambda|\,\mathrm{iter}) + O(2M\,|\mathcal{L}|\,\mathrm{iter}) + O\left(I \lg \frac{m_d}{R_{\mathrm{a}}}\,|\Lambda_i|\right) + O\left(|\mathcal{L}_m|^2\right) + O\left(M^2\right)$.

IV. SIMULATION RESULTS, ANALYSIS, AND DISCUSSION

We used the numerical data in MATLAB 2020b for the simulations to evaluate the performance of the proposed scheme. The experimental environment was an RTX 3060 GPU, i7-11700 @ 2.50GHz. The parameter values and their descriptions in the formulas related to (16) are presented in Table 1. To simulate the offshore communication environment, we exploited the wireless communication parameters referring to ocean environments [28], which are also listed in Table 1. To simulate the UAV hovering energy consumption system, we refer to the parameters and their physical meanings in [20] and [26]. The drone flight energy consumption and battery energy were obtained from [25]. The boat parameters are described in [32]. To ensure the validity of the simulation, the parameter settings were the same as those in the original study. In the ocean, 2000 sensors were deployed uniformly in an ocean plane region with 100 km^2 size. Considering that the number of sensors in our scheme is almost three times the maximum number of sensors in [24], the limited number of sensors that one UAV is responsible for collecting is set to 55, which is larger than the set of sensors (30) in [24]. Therefore, in the ocean plane region

TABLE 1. Parameters and their values.

Parameters	Value
$\mathrm{FD_L}$ [20]	11 km
$\mathrm{HT_L}$ [20]	400 s
V_{B} [32]	5 m/s
P_{B} [32]	100 kW
P_{u} [20]	212.82 W
V_{U} [26]	22 m/s
P_{c} [26]	5 W
c, d [28]	5.02, 0.35
β_0 [24]	- 40 dB
τ [26]	0.20
P_{t} [26]	23 dBm
W [28]	1 MHz
σ^2 [28]	- 114 dBm
K [24]	55
H [28]	100 m
μ [25]	58
w_0 [25]	4 m/s
h_0 [25]	10 m

above, 70 UAV hovering positions (considering redundancy) are obtained using the K-means and SEC algorithms. To illustrate the performance of MDK-LKH, we compared it with the following three algorithms:

- GANN [19]: A residual edge-graph attention (RE-GAT) neural network (GANN) was used to optimize the TEC.
- OGAA: Using original GA algorithm [10] for optimizing the TEC.
- Boat-direct scheme (BS): A boat is used to carry a UAV directly to each hovering position on the TSP route. The route was optimized using the tabu search algorithm [17].

The simulation results are the average values of 20 instances, which are analyzed and discussed as follows.

The changes in TEC under different numbers of boat waypoints are shown in Figure 4. TEC increased with an increase in the number of boat waypoints in the three schemes (our scheme, GANN, and OGAA). When there were three boat waypoints, the TECs of the three schemes had the smallest values among the waypoint number changes. When the number of boat waypoints was three to ten, our scheme exhibited the smallest TEC among the three or even four schemes. In particular, the TEC was the smallest when the number of boat waypoints was three.

For the changes in the TEC with the boat waypoint number, the algorithms and their planning were the main factors affecting the TEC by observing and comparing the three schemes with the BS scheme. The MDK-LKH and its planning resulted in the smallest TEC for the proposed scheme. In here (Figure 4), the boat-waypoint quantity is related to TEC. Compared with our scheme, the BS always requires 70 boat waypoints to collect data in the ocean data collection area. Therefore, the TEC was the highest. However, although

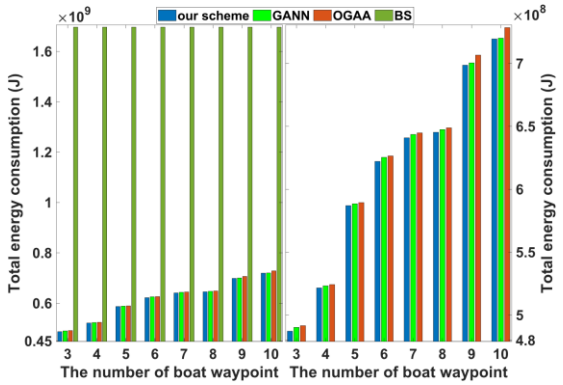

FIGURE 4. Comparison of the total energy consumption of drone and boat for the four schemes under different number of boat waypoints.

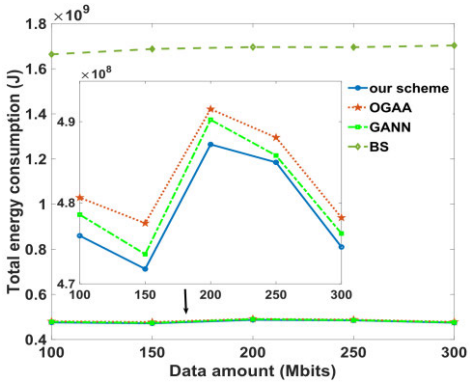

FIGURE 5. Variation in the total energy consumption of drone and boat with the data amount of the ocean environment under the four schemes.

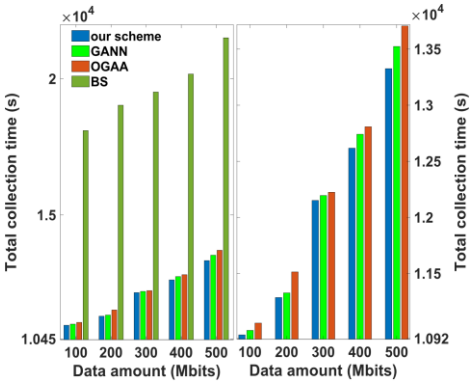

FIGURE 6. In four schemes, changes of the total data collection time of boat-assisted drone with the different data amount of the ocean environment.

GANN and OGAA have the same number of boat waypoints as our scheme, the TEC of our scheme was the smallest. In the course of optimizing the boat waypoint/hovering point and routes of boats and UAV, our scheme has a strong search capability for local and global solutions. When the number of boat waypoints is three, the TEC in our scheme is 0.03×10^8 J, 0.04×10^8 J, and 12.09×10^8 J less than that of the GANN, OGAA, and BS, respectively.

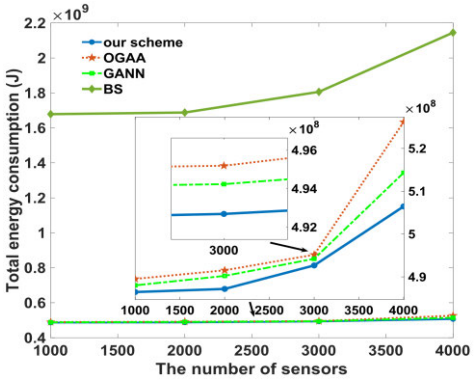

FIGURE 7. Comparing the total energy consumption of drone and boat under different sensor amount of the ocean environment in the four schemes.

TABLE 2. Summarize results.

Method	Total energy consumption in average	Total collection time in average
Our scheme	lowest	least
GANN [19]	secondary	secondary
OGAA [10]	tertiary	tertiary
IPSOA [18]	- or highest	-
ISAA [17]	- or highest	-
BS [17]	highest or -	most

Figure 5 shows the TEC variations for the four schemes. In our scheme, as the amount of data increases, the TEC first decreases, then increases, and then decreases again. This trend was also observed for the other two algorithms (OGAA and GANN). The TEC of BS increased slightly with an increase in the amount of data. By observing the energy consumption composition in Eq. (16) and the energy changes in Figure 4, we know that the use of the number of boat waypoints can impact the TEC in the course of data collection. Moreover, boat waypoint position also influenced TEC. With the advanced optimization capability of MDK-LKH, it has a higher capability of finding and optimizing boat waypoints. Therefore, our scheme always had the lowest TEC among the four schemes in the process of increasing the amount of data.

Figure 6 shows the changes in the total data collection time (Tt) with the amount of data for the four schemes. Tt increased with an increase in the amount of data, which is reasonable. However, Figures 6 and 5 show that although the sum Tt of the data collection time increases with an increase in the amount of data (Figure 6), the TEC only slightly (or not) increases with an increase in the amount of data (Figure 5). This is because the impact of the number of waypoint positions on TEC is greater than the influence of the amount of data. Owing to the excellent capability of MDK-LKH to search for local and global solutions, Tt in our scheme is the least, showing the performance of saving collection time.

We also investigated the TEC for different numbers of sensors using four schemes. Figure 7 shows that TEC is

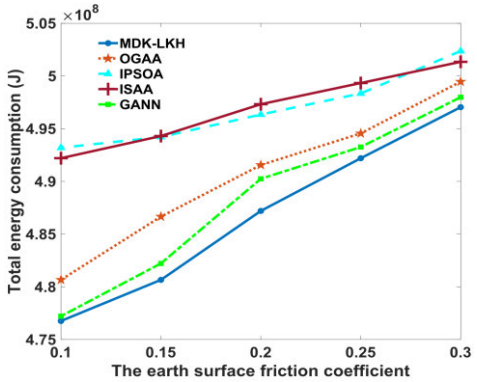

FIGURE 8. In five algorithms, changes in the total energy consumption of drone and boat with the different earth surface friction coefficient.

approximately proportional to the number of sensors. The TEC is larger because more sensors have data to collect. Under the same conditions, the TEC in our scheme was lower than that of the other three schemes. With respect to the minimum TEC, these differences became more noticeable as the number of sensors increased. In particular, for the data collection of 4000 sensors, the TEC of our scheme is only 1/4 of that of the BS scheme. This is because the LKH has a strong capability to search for local and global solutions. Therefore, our scheme can optimize the TEC of boats and UAV to the greatest extent, and the greater the number of sensors, the greater is the extent.

To fully assess the performance of MDK-LKH, we introduced two heuristic algorithms (PSO and SA) and improved them to form improved PSO algorithm (IPSOA) [18] and SA algorithm (ISAA) [17], respectively. We further studied the TEC under different Earth surface friction coefficients using the five algorithms. Figure 8 shows that the TECs is proportional to the earth's surface friction coefficient in the five algorithms. This is reasonable because the UAV energy consumption for data collection increases with an increase in Earth's surface friction coefficient. For all the coefficient conditions, MDK-LKH had the lowest TEC among the five algorithms. For example, when $\delta = 0.1$, the TEC in MDK-LKH is 0.5×10^6 J, 3.9×10^6J, 15.4×10^6 J, and 16.4×10^6 J less than that of GANN, OGAA, ISAA, and IPSOA, respectively. These results again indicate that MDK-LKH does not exhibit poor optimization characteristics.

Finally, we reviewed the total energy consumption and collection time. First, whether it is Figure 4 or Figures 5, 7, and 8, the TEC consists of four sections, i.e., which be produced in boat sailing, next, drone flying, hovering, and communicating. The TEC of Figure 4 is more representative than other figures on the total energy consumption because it involves the optimization of the boat waypoint/hovering point and the routes of boats and UAV. The four Figures show that, compared with others, our scheme does not perform poorly on the numerical values of the simulation results for four aspects: the number of boat waypoints, data amount, number of sensors, and earth surface friction coefficient. Second, Figure 6 shows a comparison of the numerical values of the simulation results of the total data collection time for the four schemes, and also shows that our scheme performs better. A conclusion showing the relatively advanced results is presented in Table 2.

V. CONCLUSION

To address the limitations of the existing scheme, this study proposes a new, time-saving, flexible, and scalable boat-supported UAV data collection scheme that aims to minimize the TEC of boats and UAV during large-scale marine sensor data collection. For this, under two constraints, a new drone hovering model, data collection and related wireless communication model are proposed, and boat and UAV route planning and their energy consumption are considered. This is followed by the formulation of the minimization TEC problem as a new special DCVRP, which is a strongly NP-hard problem. The problem is then divided into four subproblems: minimizing the sensor data collection time of the UAV, total UAV hovering energy consumption, total UAV traveling energy consumption, and boat traveling energy consumption. Therefore, this problem can be solved using the proposed MDK–KH method. The K-means algorithm was used to determine the UAV hovering positions and optimize them using the SEC algorithm. Boat waypoints are obtained using the K-means algorithm based on the hovering position. The UAV and boat routes were optimized using LKH based on the hovering positions and boat waypoints. Compared to state-of-the-art methods (GANN, OGAA, ISAA, IPSOA, and BS), the simulation results demonstrate that the proposed scheme and algorithms are capable of realizing the minimum TEC and provide time saving, scalability, and flexibility, that is, reducing the integrated cost. Under the background of the environment protection, energy saving and emission reduction idea, compared to the small-scale sensor data collection and fixed UAV charge station, our scheme can serve as a valuable reference for collecting large amounts of data from marine sensors deployed in wide and deep seas. The UAV collection of sensor data will be researched in a wider and deeper sea, and improving the security of the uploaded data by reducing the eavesdropping of uploaded information will be a future research direction.

CONFLICT OF INTEREST

The authors declare no conflict of interest.

REFERENCES

[1] G. Msigwa, J. O. Ighalo, and P.-S. Yap, "Considerations on environmental, economic, and energy impacts of wind energy generation: Projections towards sustainability initiatives," *Sci. Total Environ.*, vol. 849, pp. 157755–157766, Nov. 2022, Art. no. 157755.

[2] M. Zhang, M. Guo, R. Huang, R. Ye, Y. Li, D. Shen, and L. Wang, "Analysis of power characteristics of the offshore floating wind turbine based on the tension leg platform," in *Proc. IEEE 3rd Int. Electr. Energy Conf. (CIEEC)*, Sep. 2019, pp. 170–175.

[3] D. Kadadou, E. A. Said, R. Ajaj, and S. W. Hasan, "Research advances in nuclear wastewater treatment using conventional and hybrid technologies: Towards sustainable wastewater reuse and recovery," *J. Water Process Eng.*, vol. 52, Apr. 2023, Art. no. 103604.

[4] H. Ma, M. Shen, Y. Tong, and X. Wang, "Radioactive wastewater treatment technologies: A review," *Molecules*, vol. 28, no. 4, p. 1935, Feb. 2023.
[5] N. Kumar and J. M. Seminario, "Design of nanosensors for fissile materials in nuclear waste water," *J. Phys. Chem. C*, vol. 117, no. 45, pp. 24033–24041, Oct. 2013.
[6] L. Wei, Z. Wang, J. Liu, Z. Peng, and J.-H. Cui, "Power efficient deployment planning for wireless oceanographic systems," *IEEE Syst. J.*, vol. 12, no. 1, pp. 516–526, Mar. 2018.
[7] R. Ma, R. Wang, G. Liu, W. Meng, and X. Liu, "UAV-aided cooperative data collection scheme for ocean monitoring networks," *IEEE Internet Things J.*, vol. 8, no. 17, pp. 13222–13236, Sep. 2021.
[8] R. Ma, R. Wang, G. Liu, H.-H. Chen, and Z. Qin, "UAV-assisted data collection for ocean monitoring networks," *IEEE Netw.*, vol. 34, no. 6, pp. 250–258, Nov. 2020.
[9] H. Li, H. Wang, J. Chen, and M. Bai, "Two-echelon vehicle routing problem with time windows and mobile satellites," *Transp. Res. B, Methodol.*, vol. 138, pp. 179–201, Aug. 2020.
[10] R. G. Ribeiro, L. P. Cota, T. A. M. Euzébio, J. A. Ramírez, and F. G. Guimarães, "Unmanned-aerial-vehicle routing problem with mobile charging stations for assisting search and rescue missions in postdisaster scenarios," *IEEE Trans. Syst., Man, Cybern., Syst.*, vol. 52, no. 11, pp. 6682–6696, Nov. 2022.
[11] A. K. W. Chee, R. F. Broom, C. J. Humphreys, and E. G. T. Bosch, "A quantitative model for doping contrast in the scanning electron microscope using calculated potential distributions and Monte Carlo simulations," *J. Appl. Phys.*, vol. 109, no. 1, pp. 1–9, Jan. 2011.
[12] P.-Q. Huang, Y. Wang, K. Wang, and K. Yang, "Differential evolution with a variable population size for deployment optimization in a UAV-assisted IoT data collection system," *IEEE Trans. Emerg. Topics Comput. Intell.*, vol. 4, no. 3, pp. 324–335, Jun. 2020.
[13] D. N. Das, R. Sewani, J. Wang, and M. K. Tiwari, "Synchronized truck and drone routing in package delivery logistics," *IEEE Trans. Intell. Transp. Syst.*, vol. 22, no. 9, pp. 5772–5782, Sep. 2021.
[14] A. G. H. Kek, R. L. Cheu, and Q. Meng, "Distance-constrained capacitated vehicle routing problems with flexible assignment of start and end depots," *Math. Comput. Model.*, vol. 47, nos. 1–2, pp. 140–152, Jan. 2008.
[15] J. Zheng, K. He, J. Zhou, Y. Jin, and C.-M. Li, "Reinforced Lin–Kernighan–Helsgaun algorithms for the traveling salesman problems," *Knowl-Based Syst.*, vol. 260, Jan. 2023, Art. no. 110144.
[16] K. Helsgaun, "General k-opt submoves for the Lin–Kernighan TSP heuristic," *Math. Program. Comput.*, vol. 1, nos. 2–3, pp. 119–163, Jul. 2009.
[17] S. Han, K. Zhu, M. Zhou, and X. Liu, "Joint deployment optimization and flight trajectory planning for UAV assisted IoT data collection: A bilevel optimization approach," *IEEE Trans. Intell. Transp. Syst.*, vol. 23, no. 11, pp. 21492–21504, Nov. 2022.
[18] M. S. Sarbijan and J. Behnamian, "Multi-fleet feeder vehicle routing problem using hybrid metaheuristic," *Comput. Oper. Res.*, vol. 141, May 2022, Art. no. 105696.
[19] K. Lei, P. Guo, Y. Wang, X. Wu, and W. Zhao, "Solve routing problems with a residual edge-graph attention neural network," *Neurocomputing*, vol. 508, pp. 79–98, Oct. 2022.
[20] H.-M. Chung, S. Maharjan, Y. Zhang, F. Eliassen, and K. Strunz, "Placement and routing optimization for automated inspection with unmanned aerial vehicles: A study in offshore wind farm," *IEEE Trans. Ind. Informat.*, vol. 17, no. 5, pp. 3032–3043, May 2021.
[21] D. Xu, Y. Sun, D. W. K. Ng, and R. Schober, "Multiuser MISO UAV communications in uncertain environments with no-fly zones: Robust trajectory and resource allocation design," *IEEE Trans. Commun.*, vol. 68, no. 5, pp. 3153–3172, May 2020.
[22] H. Luo, Z. Liang, M. Zhu, X. Hu, and G. Wang, "Integrated optimization of unmanned aerial vehicle task allocation and path planning under steady wind," *PLoS ONE*, vol. 13, no. 3, Mar. 2018, Art. no. e0194690.
[23] M. Coombes, T. Fletcher, W. Chen, and C. Liu, "Decomposition-based mission planning for fixed-wing UAVs surveying in wind," *J. Field Robot.*, vol. 37, no. 3, pp. 440–465, Apr. 2020.
[24] B. Xu, L. Zhang, Z. Xu, Y. Liu, J. Chai, S. Qin, and Y. Sun, "Energy optimization in multi-UAV-assisted edge data collection system," *Comput., Mater. Continua*, vol. 69, no. 2, pp. 1671–1686, 2021.
[25] R. T. Palomaki, N. T. Rose, M. van den Bossche, T. J. Sherman, and S. F. J. De Wekker, "Wind estimation in the lower atmosphere using multirotor aircraft," *J. Atmos. Ocean. Technol.*, vol. 34, no. 5, pp. 1183–1191, May 2017.
[26] Y. Zeng, J. Xu, and R. Zhang, "Energy minimization for wireless communication with rotary-wing UAV," *IEEE Trans. Wireless Commun.*, vol. 18, no. 4, pp. 2329–2345, Apr. 2019.
[27] L. Wang, H. Zhang, S. Guo, and D. Yuan, "Deployment and association of multiple UAVs in UAV-assisted cellular networks with the knowledge of statistical user position," *IEEE Trans. Wireless Commun.*, vol. 21, no. 8, pp. 6553–6567, Aug. 2022.
[28] Y. Wang, W. Feng, J. Wang, and T. Q. S. Quek, "Hybrid satellite-UAV-terrestrial networks for 6G ubiquitous coverage: A maritime communications perspective," *IEEE J. Sel. Areas Commun.*, vol. 39, no. 11, pp. 3475–3490, Nov. 2021.
[29] A. Al-Hourani, S. Kandeepan, and S. Lardner, "Optimal LAP altitude for maximum coverage," *IEEE Wireless Commun. Lett.*, vol. 3, no. 6, pp. 569–572, Dec. 2014.
[30] M. Mozaffari, W. Saad, M. Bennis, and M. Debbah, "Mobile unmanned aerial vehicles (UAVs) for energy-efficient Internet of Things communications," *IEEE Trans. Wireless Commun.*, vol. 16, no. 11, pp. 7574–7589, Nov. 2017.
[31] W. Wang, W. P. Wang, and J. W. Wang, "An algorithm for finding the smallest circle containing all points in a given point set," *J. Softw.*, vol. 11, no. 9, pp. 1237–1240, Sep. 2000.
[32] Y.-K. Son, S.-Y. Lee, and S.-K. Sul, "DC power system for fishing boat," in *Proc. IEEE Int. Conf. Power Electron., Drives Energy Syst. (PEDES)*, Dec. 2018, pp. 1–6.

XIANFEI HUANG received the M.Sc. degree in software engineering from Guangxi University, Guangxi, China, in 2018, where he is currently pursuing the Ph.D. degree in electrical engineering. His research interests include the routing algorithms, various optimization, and performance evaluation.

GAOCAI WANG received the Ph.D. degree in computer science from Central South University, China, in 2004. Afterwards, he went to Tsinghua University, University of Toledo, and Texas Southern University as a Postdoctoral Researcher. He is currently a Professor with the Department of Computer Science, Guangxi University. His research interests include computer networks, routing algorithms, and performance evaluation.